Proceedings of the 21st ICSMGE, Vienna, Austria, 14 – 19 June 2026. Pistrol, Adam & Schweiger (eds.)
Published by: ÖGG, Austrian Society for Geomechanics, Salzburg, Austria, ISBN 978-3-9503898-4-5
https://doi.org/10.53243/ICSMGE2026-1397

Approaches for seismic soil-structure interaction analysis of a railway bridge pier on pile foundations

Pierluigi Alesiani, Paolo Ruggeri
Department SIMAU, Università Politecnica delle Marche, Ancona, Italy, p.alesiani@staff.univpm.it

Giuseppe Scarpelli
GES-Geotechnical Engineering Services, Italy (formerly Università Politecnica delle Marche, Ancona, Italy)

Michele di Tullio, Angelo Lambrughi, Nicola Valiante, Marco Orlandini
Webuild, Milan, Italy

ABSTRACT: Soil-Structure Interaction (SSI) effects are often neglected in the current design practice of bridge superstructures and foundations. This simplification generally results in overestimating seismic actions, although underestimations may also occur in some cases. This study investigates SSI effects on a bridge pier supported by pile foundations, using a high-speed railway viaduct as a case study. Two approaches are carried out: a "direct" approach and a "substructure" approach, both capable of simulating SSI. The direct approach is based on a direct-integration time-history analysis of a three-dimensional finite element model (FEM) of the global system (i.e. soil-foundation-structure), in which the nonlinear behavior of the soil is described using an elastoplastic constitutive law with hardening and hysteretic properties. The substructure approach, on the other hand, is based on a visco-elastic lumped parameters model (LPM) described in the literature. This model consists of an assemblage of masses, elastic springs and dampers capable of reproducing the dynamic impedances of the soil-foundation system. The results from these two approaches, carried out using site-specific ground motions, are finally compared with those of a simplified design method compliant with the Italian building code, which neglects the seismic interaction and is based on linear dynamic (response spectrum) analysis of the fixed-base single-degree-of-freedom system.

KEYWORDS: Seismic Soil-Structure Interaction, 3D FEM, HSsmall, LPM, bridge pier, pile foundation.

1 INTRODUCTION

The advancement of computing systems and the development of constitutive models suitable for nonlinear dynamic finite element analyses now make it feasible to explore the behavior of engineering structures and infrastructure through 3D numerical simulations. It is therefore interesting to compare the conventional design approach commonly used in engineering practice with more advanced analyses capable of accounting for soil-foundation-structure interaction (SFSI).

The design of bridges and viaducts on pile foundation is typically carried out using fixed-base structural models that completely ignore the compliance and energy dissipation by radiation of the foundation system. Moreover, when using the ground classification criteria prescribed by national building codes, the modification of the seismic input caused by local site effects and by kinematic soil-foundation interaction is only approximately taken into account. These simplifications are generally considered acceptable, as they usually lead to higher structural demands and, consequently, conservative design solutions. However, there are cases where SFSI can increase the seismic demand (Milonakis & Gazetas, 2000; de Sanctis & Di Laora, 2016), for example due to lengthening of the fundamental period or resonance phenomena with the natural vibration period of the soil deposit. In either way, it appears equally important to include SFSI in the analysis model in order to assess the actual margin of safety. A realistic assessment of the seismic behavior of the structure allows more informed design choices, optimization of structural elements, and a more efficient use of economic resources allocated to its construction.

This paper presents the seismic analysis of a pier on pile foundation of a high-speed railway viaduct located in the Venetian plain, using a 3D finite element model aimed at evaluating the soil-foundation-structure interaction (direct approach), also considering local site effects. The results of this advanced but computationally demanding analysis are compared with those obtained from a simpler visco-elastic lumped parameter model (substructure approach), which can nonetheless capture some aspects of SFSI, and with the typical design approach based on a structural fixed-base model and the elastic response spectrum.

2 GEOTECHNICAL MODEL AND STRUCTURE

2.1 *Geology and geotechnical-seismic model*

The Venetian Plain is a complex alluvial deposit formed during the Quaternary period by the infill of a large depression in the Tertiary basement. The architecture of the deposit is controlled by the interaction between major river systems (Po and Adige rivers) and the succession of glacial and interglacial periods, which caused significant sea-level fluctuations and changes in river courses. As a result, the alluvial formation consists mainly of continental deposits whose grain size becomes progressively finer with increasing distance from the mountains.

For the development of the geotechnical–seismic model, this classification is particularly useful as it helps identify the areas where cohesive layers have a significant areal continuity. The study area is located in the Middle Venetian Plain, where alternating fluvial and overbank processes produced laterally extensive clayey layers interbedded with gravelly channel deposits; therefore, for seismic wave propagation analyses, it is appropriate to consider the sequence of cohesive and granular layers that characterize the deposit.

Nonetheless, for the reasons above the site exhibits a significant variability in layers thickness along a vertical section, as shown by the two boreholes and Vs profiles in Figure 1. This lateral heterogeneity was generalized into a simplified stratigraphic profile (Table 1), which was adopted for the dynamic analyses with the aim of catching the overall seismic site response.

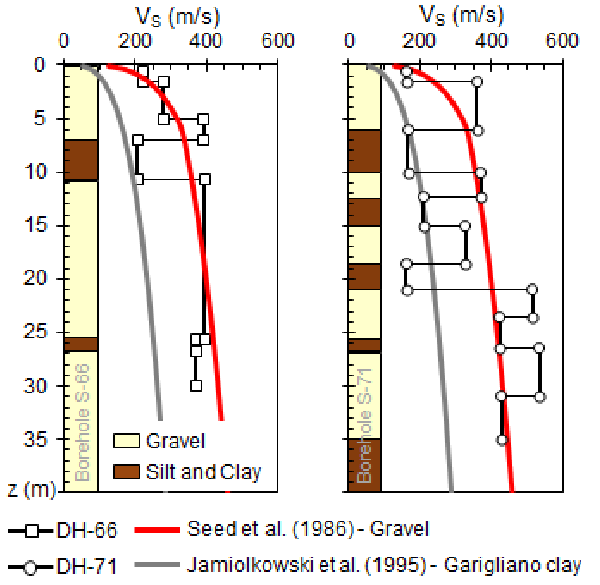

Figure 1. VS profiles with depth from Down-Hole tests and literature.

The shear wave velocities measured through Down-Hole tests are consistent with the trends proposed by Seed et al. (1986) for gravel and Jamiolkowski et al. (1995) for clay. Based on the $V_{S,30}$ value, the site ground type is C. The shear modulus decay curves and damping ratio curves with shear strain adopted in this study are those proposed by Rollins et al. (2020) for gravel layers and Vucetic & Dobry (1991) for silt and clay layers.

The seismic bedrock was assumed at a depth of 100 m below the ground surface, based on the inversion of ambient vibration measurements, hydrogeological considerations and parametric site response analyses.

2.2 *Structure description*

The viaduct is part of the Verona-Vicenza-Padova high-speed/high-capacity railway line and consists of simply supported spans with a length of 25 m and a prestressed concrete deck. The typical pier analyzed (Figure 2) consists of a hollow rectangular reinforced concrete shaft, 10.50 m in height, supported by a foundation cap measuring 12.0×12.0×2.50 m resting on nine piles with a diameter of 1.50 m and a length of 36.0 m. Considering the seismic load combinations, the vertical load transferred to each pier by the deck is 12,840 kN, while the pier shaft and cap contribute additional 3,850 kN.

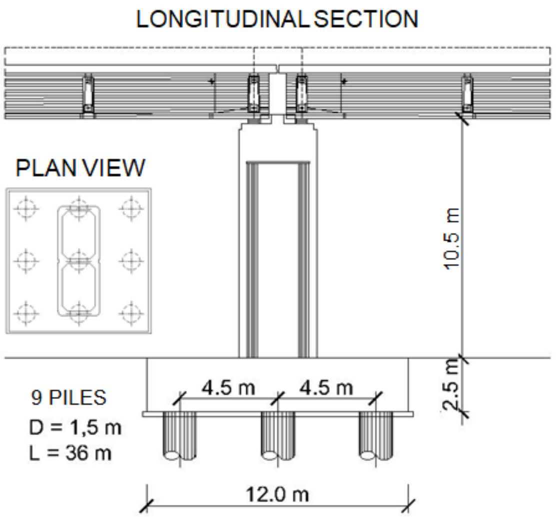

Figure 2. Longitudinal cross-section and plan view of the pier.

In the simplified fixed-base single-degree-of-freedom model, the fundamental vibration period is T_l = 0.30 s in the longitudinal direction and T_t = 0.16 s in the transverse direction.

3 SITE RESPONSE ANALYSIS (SRA)

3.1 *Seismic input*

The seismic action was defined from the site-specific seismic hazard at rock site defined by the Italian building code for a return period of 1424 years, selecting seven pairs of natural, spectrum-compatible accelerograms to study separately the two main loading directions of the pier (longitudinal and transverse to the railway route).

Using the ESM database (https://esm-db.eu), the time histories were manually selected following good practice criteria, considering magnitude (M=5.00-6.50) and distance (R=2-62 km) ranges representative of the site's seismicity, recordings on outcropping bedrock or stiff soil ($V_S \geq 662$ m/s), and moderate scale factors (0.60-1.80).

The average spectrum-compatibility is satisfied both for the two sets of seven accelerograms (EO components for the longitudinal direction, NS components for transverse direction) and for the combination of all fourteen horizontal components, computed by averaging the SRSS (square-root of sum of squares) spectra of each pair of registrations. Figure 3 shows the elastic response spectra (5% damping) of the seven accelerogram applied in longitudinal direction, along with the average and target (ground type A) spectra.

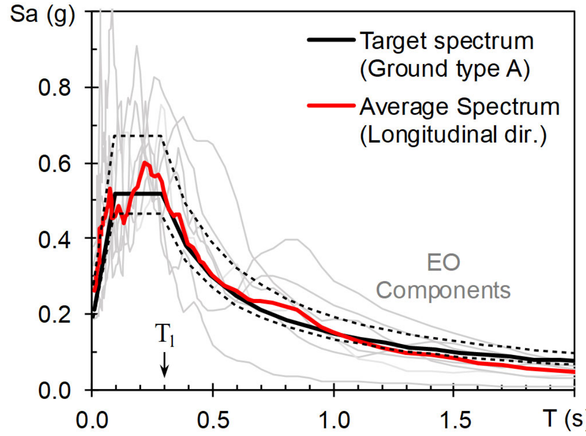

Figure 3. Elastic response spectra and spectrum-compatibility check.

3.2 *Equivalent Linear model*

The equivalent-linear site response (EQ-L) was carried out using total stress analysis in the frequency domain with the STRATA software (Kottke & Rathje, 2009). The properties of the 1D soil model analyzed are those of Table 1.

Table 1. Simplified stratigraphic model adopted in the analyses.

Soil	z (m)	V_S (m/s)	G/G_0 and D
Gravel	0.0-4.5	300	Rollins et al. – p'=100 kPa
Silt/Clay	4.5-8.5	138-150	Vucetic & Dobry – PI=30
Gravel	8.5-17.5	320-350	Rollins et al. – p'=100 kPa
Silt/Clay	17.5-24.5	190-200	Vucetic & Dobry – PI=30
Gravel	24.5-29.5	402	Rollins et al. – p'=100 kPa
Silt/Clay	29.5-33.5	200	Vucetic & Dobry – PI=30
Gravel	33.5-41.5	431-443	Rollins et al. – p'=100 kPa
Silt/Clay	41.5-45.5	200	Vucetic & Dobry – PI=30
Gravel	45.5-100	487-546	Rollins et al. – p'=350 kPa
Bedrock	> 100.0	800	–

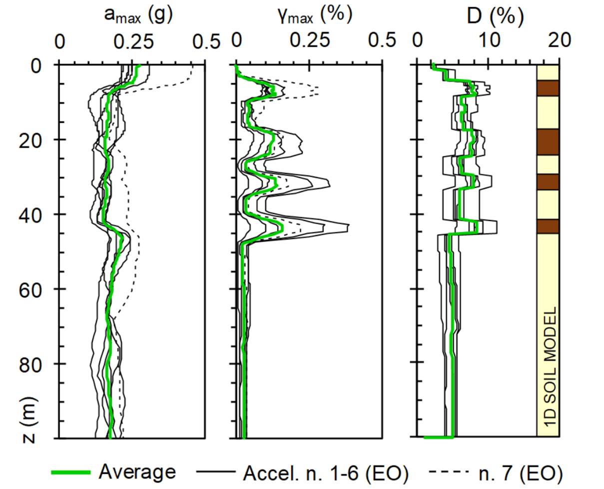

Figure 4. EQ-L site response analysis results. Profiles of maximum acceleration, maximum shear strain and mobilized damping ratio.

The output included the site-specific free-field ground motions at surface and mobilized soil stiffness at various depths, depending on the shear strain levels induced by the earthquakes.

Assuming the stratigraphic model reported in Table 1 and using the seven EO acceleration components arbitrarily assigned to the pier's longitudinal direction, Figure 4 presents the profile with depth of maximum acceleration (a_{max}), maximum shear strain (γ_{max}) and mobilized damping ratio (D). The average profiles highlight a marked increase in acceleration in the first 10 m below the surface and concentration of shear strain in the clay layers, especially in depth, where significant damping occurs.

The average maximum shear strain is about 0.10-0.20%, generally acceptable for the reliability of the EQ-L method, except for a few stronger records that induce larger strains.

4 SEISMIC INTERACTION ANALYSIS

4.1 *3D finite element model (3D FEM)*

Dynamic interaction was first analyzed with the direct approach using a 3D finite element model of the whole soil-foundation-structure system, built in PLAXIS 3D (Bentley, 2023). For computational efficiency, only half the system was modeled, exploiting geometric and loading symmetry. The model extends 300×30 m in plan and 100 m in depth (down to the seismic bedrock) and includes about 270,000 finite elements (Figure 5).

The superstructure was modeled as a single-degree-of-freedom oscillator, using a linear visco-elastic beam element 11.0 m long with all seismic mass concentrated at the top. The cross-section properties account for cracked concrete stiffness and 5% Rayleigh damping. The foundation cap and piles were modeled with 10-node tetrahedral volume elements with uncracked concrete stiffness and 2.5% Rayleigh damping. The clay and gravel layers were discretized with tetrahedral elements assigning the HSsmall elasto-plastic constitutive model (Benz et al. 2007), which captures nonlinear and hysteretic soil behavior (adopted parameters in Table 2).

A wide model extension in the loading direction (X axis) was needed to reduce boundary effects during dynamic phases, due to limitations in coupling the free-field boundary with the HSsmall material. To minimize this disturbance, non-collapsible side zones (named "high shear strength soil column") were added to avoid unwanted plastic failure mechanisms at the edges. Average stiffnesses values were assumed within these zones (i.e. m = 0) and the hysteretic behavior was preserved adopting the same constitutive model of the adjacent soil. A tensile strength and cohesion of 200 kPa were found to be sufficient to prevent collapse. The influence of these side zones is therefore limited to stabilizing the numerical response at lateral boundaries in order to preserve the intended dynamic behavior within the central region.

The seismic horizontal load was applied at the model base using the "compliant base" boundary condition as an equivalent shear stress, derived by deconvolving the input motion from the 1D EQ-L model. The 3D model described above, which includes the soil, foundation and structure, makes it possible to obtain the dynamic response of the complete system, which depends on the local site response as well as on kinematic and inertial interaction effects.

Table 2. HSsmall soil model parameters.

Parameter	Unit of measure	Gravel	Silt/Clay
γ	kN/m^3	19.0	19.0
G_0^{ref}	kN/m^2	33000	7000
$\gamma_{0.7}$	%	0.01	0.05
υ_{ur}	–	0.2	0.2
E_{50}^{ref}	kN/m^2	65000	4800
E_{oed}^{ref}	kN/m^2	65000	3400
E_{ur}^{ref}	kN/m^2	162500	24000
p^{ref}	kN/m^2	100	100
m	–	0.5	0.6
c'	kN/m^2	1	5
φ'	°	39	26

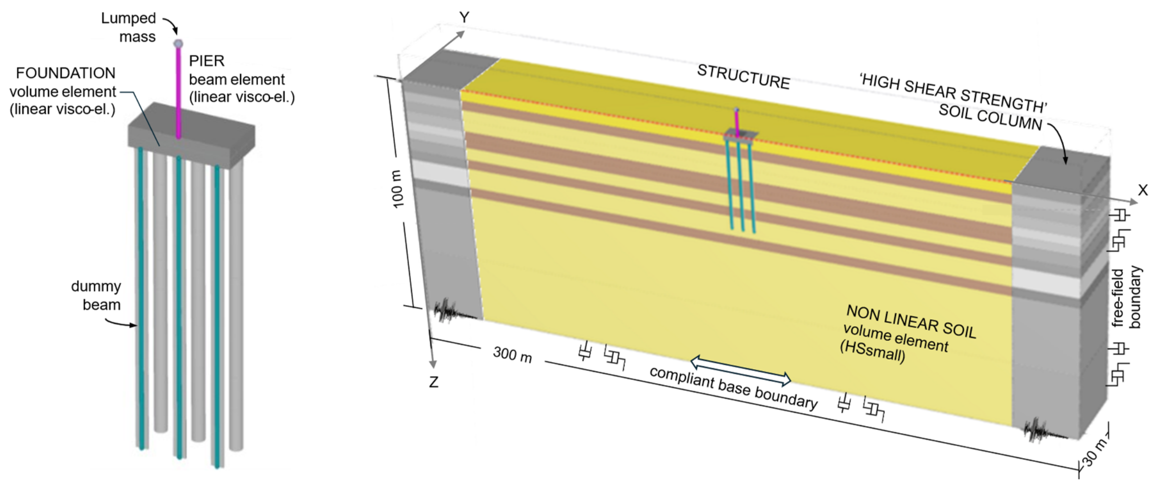

Figure 5. Scheme of the 3D finite element model for the soil-foundation-structure interaction analysis. Modified after Alesiani et al. (2025).

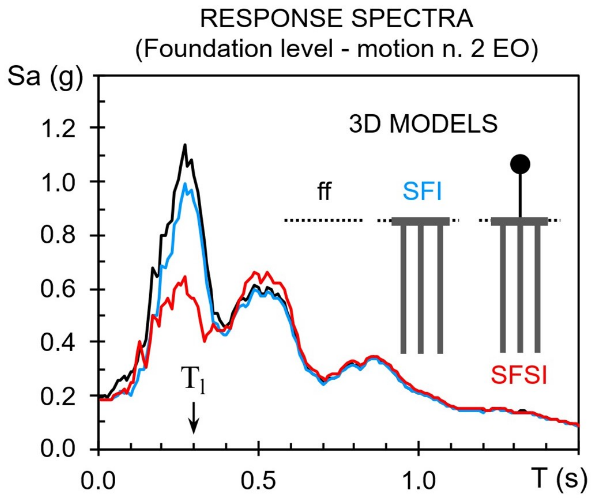

Figure 6. 3D finite element analysis. Elastic response spectra (ξ=5%) at the foundation level obtained for the three models: ff, SFI and SFSI.

To assess the contribution of each component, the results of the complete model (SFSI) were compared with: (i) a model including only the soil layers (ff), to evaluate the nonlinear (NL) site response; and (ii) a model with the soil, foundation cap and piles (SFI), but without the superstructure, to evaluate the seismic motion at the foundation level and so the kinematic interaction.

Figure 6 shows, for the horizontal EO component of a representative accelerogram, the elastic response spectra at the foundation level obtained from the three considered finite element models. For this specific case study, it can be seen that the filtering effect of the foundation alone on the free-field ground motion is modest. By contrast, the combined effects of kinematic and inertial interaction are much more significant, as clearly highlighted by the ratio of the spectral ordinates of the complete system motion to those of the free-field ground motion ($S_{e,SFSI}/S_{e,ff}$), showing a reduction in spectral acceleration of up to 40% around the fundamental vibration period of the system (Figure 7).

The spectral acceleration ratio for the soil-foundation interaction model ($S_{e,SFI}/S_{e,ff}$) is also reported in Figure 7 for comparison, together with the spectral ratio curve proposed by Di Laora & de Sanctis (2013) to account for kinematic interaction of pile foundation. The literature curve corresponds to the upper bound of homogeneous soil deposit case, computed using the average mobilized shear stiffness derived from the EQ-L site response analysis.

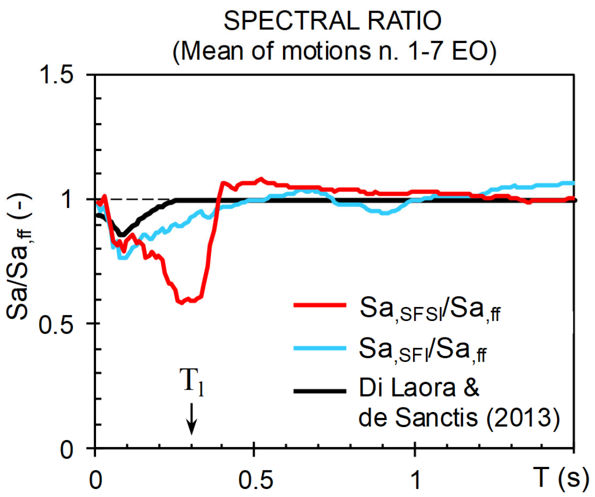

Figure 7. Mean spectral acceleration ratio (longitudinal direction).

4.2 *Lumped parameter model (LPM)*

Concerning substructure approach, the inertial interaction analyses were performed using a visco-elastic lumped parameter model (LPM) as proposed by Carbonari et al. (2018), which approximates the dynamic stiffness of the pile group through an assemblage of frequency-independent parameters: masses (m_i), elastic springs (k_i) and viscous dampers (c_i). A scheme of the model and its parameters is shown in Figure 8. The eccentric components, connected to the master node by rigid elements (link) of different lengths, allow to catch the coupling between rotation and translation in horizontal directions.

The dynamic response of the LPM is decoupled in the horizontal x and y directions, as well as in the vertical and torsional degrees of freedom. In this application, only the response to horizontal seismic loading was considered. The resulting impedance matrix components K_{ij} have a real part varying quadratically and an imaginary part varying linearly with the angular frequency ω:

$$K_{ij}(\omega) = Re(K_{ij}) + Im(K_{ij})$$
$$K_{ij}(\omega) = (k_{ij} - \omega^2 m_{ij}) + jc_{ij}\omega \qquad (1)$$

The dynamic impedances of the soil-foundation system as a function of frequency were obtained using the commercial software DynaPile (Ensoft Inc., 2019), which is based on the "consistent boundary matrix method" (Blaney et al., 1976). The piles were assumed to be rigidly connected at the head, and visco-elastic soil properties (stiffness and damping ratio) corresponding to the average shear strain levels from the EQ-L analysis (Figure 4) were adopted. As shown in Figure 9, the lumped parameters were calibrated using least squares fitting to match the actual dynamic impedances in the frequency range of interest (f = 0-10 Hz).

To preserve the simplicity of the substructure approach, the acceleration time histories used as input in the LPM were those from the EQ-L analysis, taken at pile head depth and modified by the group transfer function to obtain the foundation input motion (FIM). Consistent with the 3D finite element SFI model results (Figure 7), kinematic interaction effects are minor, so the foundation motion may be assumed equal to the free-field ground motion without significant errors.

Finally, the inertial interaction analyses were carried out assembling the LPM in SAP2000, modeling the superstructure as a linear elastic single-degree-of-freedom oscillator and using a Newmark direct time-domain integration with 5% viscous damping proportional to stiffness.

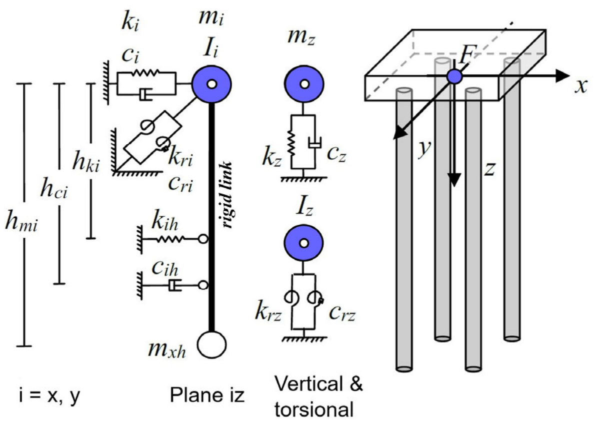

Figure 8. Assemblage of LPM. Modified after Carbonari et al. (2018).

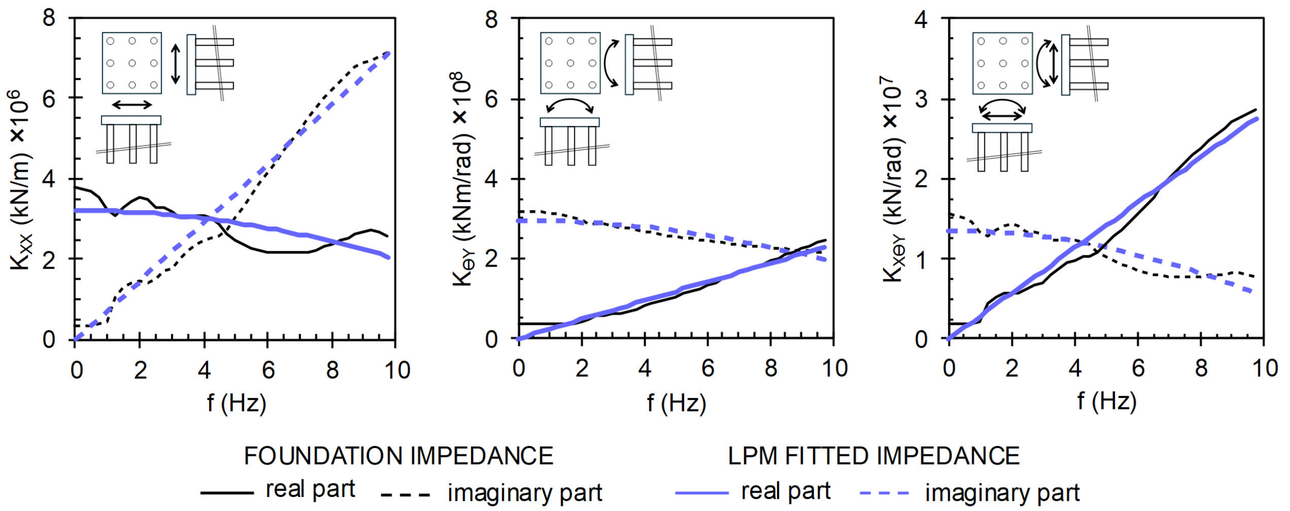

Figure 9. Impedance functions of the pile foundation: translational (K_{XX}), rotational ($K_{\theta Y}$) and coupled roto-translational ($K_{X\theta Y}$).

5 FIXED-BASE MODEL (FB)

The benchmark results for evaluating seismic SSI effects are those obtained from the fixed-base (FB), linear elastic single-degree-of-freedom (SDoF) model of the individual pier. This idealization is justified, as the railway viaduct consists of simply supported spans. Moreover, most of the seismic mass is concentrated at the pier head, making higher vibration modes involving the pier shaft negligible. The hypothesis of a fixed base is more questionable, but it is usually adopted in current practice for piers on pile foundation.

In compliance with the Italian building code (MIT, 2018), the design seismic action is obtained from a linear dynamic analysis using the elastic design response spectrum (Figure 10). As discussed above, this approach involves two main simplifications:

1. the local site response is approximated by means of the soil factor, which depends on the ground type;
2. the foundation compliance is neglected.

In order to assess the influence of these simplifications, the design response spectrum for ground type C will be compared with the average spectra from the site response analyses, and the maximum shear force at the pier base obtained from the FB model will be compared with those from the 3D FEM and LPM analyses which include interaction effects.

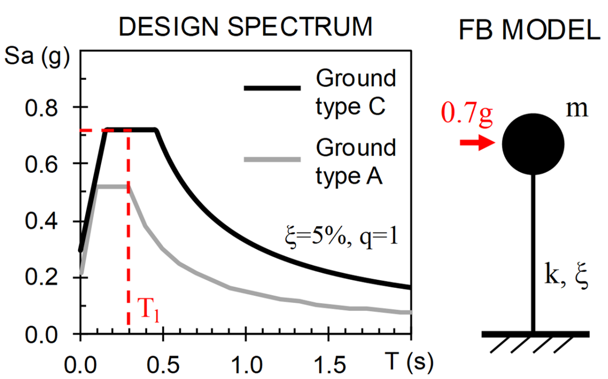

Figure 10. Scheme of the fixed-base model (FB) and elastic design response spectrum as defined by the Italian building code.

6 RESULTS

6.1 *Contribution of site response*

The reduction of the seismic actions obtained by taking into account site-specific ground motions is shown in Figure 11c, where the average response spectrum, computed from the 7 accelerograms in longitudinal direction (ξ=5%), is compared to the design spectrum for ground type C. At the fundamental vibration period of the fixed-base model (T_1 = 0.30 s), the spectral acceleration is reduced by 5% for the L-EQ model and by 18% for the NL model, respectively. An additional reduction of seismic action is expected due to period lengthening and damping effects induced by the foundation compliance. Nevertheless, a proper evaluation for design purposes should be based on regularized spectra, to remove the influence of peaks and valleys in the spectral acceleration resulting from the selection of natural ground motions.

6.2 *Comparison between models*

Figure 12 shows, for the longitudinal direction, the maximum base shear force (V_{max}) obtained from the 3D FEM (SFSI model) and LPM analysis. The results of the two analyses are very similar, although some differences appear for the most intense earthquakes, like motion n. 7. In these cases, the complete model shows a more damped structural response due to greater nonlinear soil mobilization during seismic propagation. This is evident by comparing the NL site response analysis with the EQ-L analysis from which the LPM input time histories are derived. In fact, from Figure 11ab it can be observed that for record n. 7, the L-EQ method overestimates the spectral acceleration around the fundamental vibration period compared to the NL analysis. Apart from this specific motion, the average spectra from both analyses are similar and slightly lower than the code spectrum for ground type C. This again underscores the importance of an accurate evaluation of local site response during the design phase.

From the comparison of the 3D FEM analysis with the fixed-base approach (Figure 13), it is possible to appreciate the significant contribution of dynamic soil-foundation-structure interaction effects. For the considered case study, SFSI led to a more damped pier response (due to radiation and hysteresis), reducing the maximum base shear by about 30%. Similar results (not shown herein for brevity) were obtained in the transverse direction.

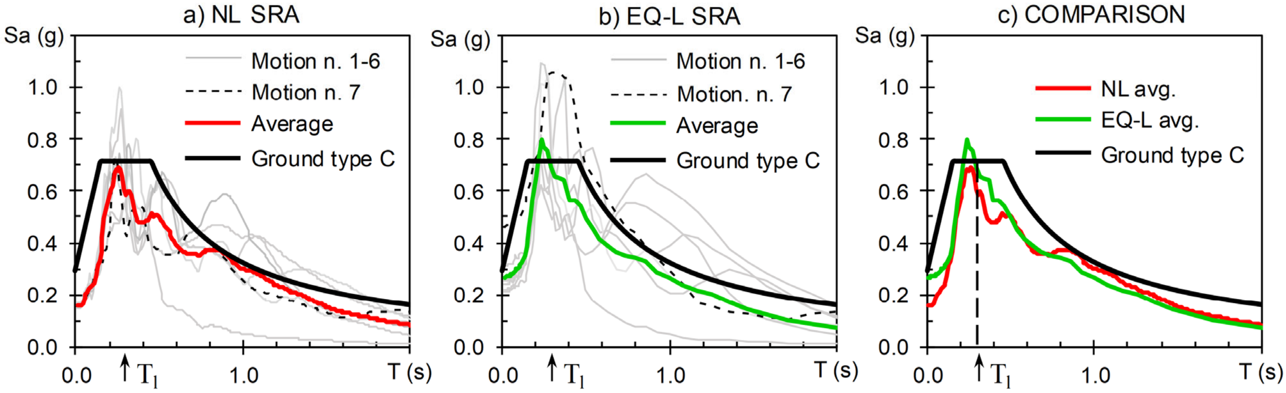

Figure 11. Elastic response spectra (ξ=5%) from site response analyses with equivalent linear (EQ-L) and non-linear (NL) models (longitudinal direction). Comparison with the code design spectrum for ground type C.

7 CONCLUSIONS

The 3D FEM SFSI analyses provide a realistic assessment of seismic behavior, with potentially significant design implications. Their adoption in infrastructure design practice should be encouraged, despite some practical complexity. In this context, using site-specific ground motions instead of the code design spectrum further enhances the accuracy of the analysis by capturing local site effects. Also, the simpler LPM approach appears promising, as it can effectively capture the main interaction effects under moderate seismic events. However, under strong earthquakes, this visco-elastic approach shows some limitations, as it cannot fully account for the mobilization of soil and structure non-linearity. Further studies are ongoing to refine the method for application under such conditions.

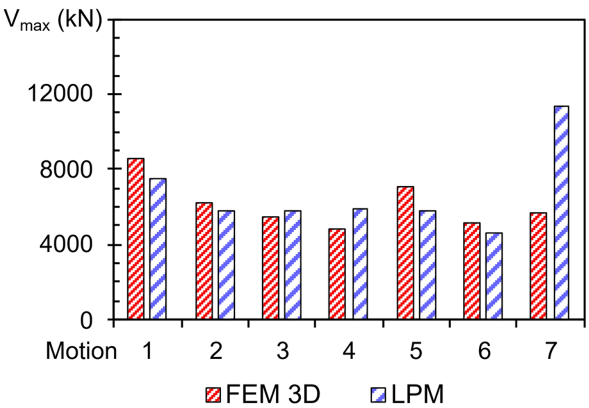

Figure 12. Results of seismic SFSI analysis (longitudinal direction). Maximum base shear force obtained from 3D FEM and LPM models.

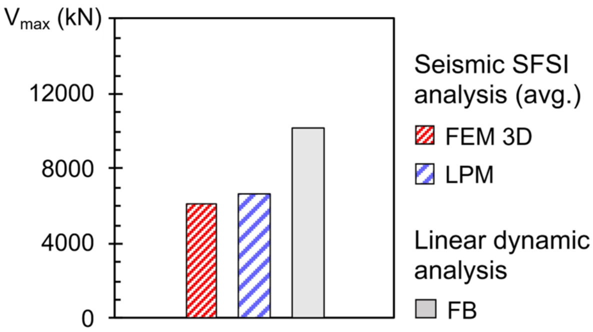

Figure 13. Comparison between seismic SFSI analyses (3D FEM, LPM) and linear dynamic analysis of the fixed-base model (FB).

8 REFERENCES

Alesiani, P., Ruggeri, P., Scarpelli, G., Di Tullio, M., Lambrughi, A., Valiante, N., Orlandini, M. 2025. Analisi dinamica agli elementi finiti di una pila isostatica fondata su pali per un viadotto dell'Alta Velocità ferroviaria. In *Sicurezza, manutenzione e sviluppo delle infrastrutture - XXVIII Convegno Nazionale di Geotecnica*, Venice, ISBN 9788855536660: AGI.

Bentley, 2023. PLAXIS 3D V23.2.

Benz, T., Vermeer, P. A., and Schwab, R. 2009. A small-strain overlay model. International journal for numerical and analytical methods in geomechanics, 33(1), 25-44.

Blaney, G., Kausel, W. & Roësset, J. M. 1976. Dynamic stiffness of piles. In *Proceedings of the 2nd International Conference on Numerical Methods in Geomechanics,* 1001-1012. ASCE.

Carbonari, S., Morici, M., Dezi, F., and Leoni, G. 2018. A lumped parameter model for time-domain inertial soil-structure interaction analysis of structures on pile foundations. *Earthq. Eng. Struct. Dyn., 47*(11).

de Sanctis, L., and Di Laora, R. 2016. Importance of kinematic interaction in the seismic vulnerability assessment of pile-supported buildings. *Rivista Italiana di Geotecnica*, *51*(4), 47-59.

Di Laora, R., and de Sanctis, L. 2013. Piles-induced filtering effect on the foundation input motion. *Soil Dynamics and Earthquake Engineering*, *46*, 52-63.

Ensoft Inc, 2019. DynaPile 2016.

Kottke, A. R., & Rathje, E. M. 2009. Technical manual for Strata. Berkeley, California: PEER.

Jamiolkowski, M., Lancellotta, R., & Lo Presti, D. C. 1995. Remarks on the stiffness at small strains of six Italian clays. In P*re-failure deformation of geomaterials*, Sapporo. Rotterdam: Balkema.

MIT, 2018. D.M. del Ministero delle Infrastrutture e dei trasporti del 17/01/2018. Aggiornamento delle Norme Tecniche per le Costruzioni. NTC 2018 (in Italian).

Mylonakis, G., and Gazetas, G. 2000. Seismic soil-structure interaction: beneficial or detrimental? *Journal of Earthquake Engineering*, 4(3), 277-301.

Rollins, K. M., Singh, M., & Roy, J. 2020. Simplified equations for shear-modulus degradation and damping of gravels. *Journal of Geotechnical and Geoenvironmental Engineering*, *146*(9).

Seed, H. B., Wong, R. T., Idriss, I. M., & Tokimatsu, K. 1986. Moduli and damping factors for dynamic analyses of cohesionless soils. *Journal of geotechnical engineering*, *112*(11), 1016-1032.

Vucetic, M., and Dobry, R. 1991. Effect of soil plasticity on cyclic response. *Journal of Geotechnical Engineering*, *117*(1), 89-107.